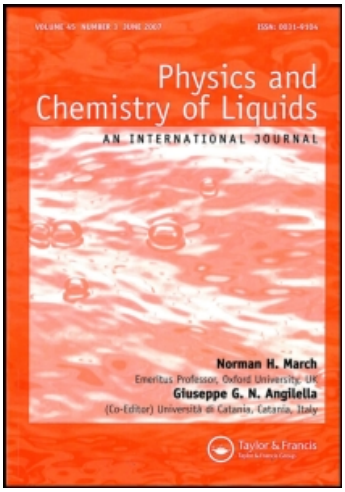

Physics and Chemistry of Liquids
Publication details, including instructions for authors and subscription information:
http://www.informaworld.com/smpp/title~content=t713646857

Density and ion size effects in polarisable models of molten KI

M. Dixon[a]; M. J. L. Sangster[a]
[a] J. J. Thomson Physical Laboratory, University of Reading, Whiteknights

To cite this Article Dixon, M. and Sangster, M. J. L.(1976) 'Density and ion size effects in polarisable models of molten KI', Physics and Chemistry of Liquids, 5: 3, 221 — 236
To link to this Article: DOI: 10.1080/00319107608084120
URL: http://dx.doi.org/10.1080/00319107608084120

Phys. Chem. Liq., 1976, Vol. 5, pp. 221–236

Printed in Dordrecht, Holland

Density and Ion Size Effects in Polarisable Models of Molten KI

M. DIXON and M. J. L. SANGSTER
J. J. Thomson Physical Laboratory, University of Reading, Whiteknights, Reading RG6 2AF

A method for generating interionic potentials from solid state data including ionic radii is presented. A set of potentials with different ion sizes is fitted to KI data and the changes in some of the static and dynamic properties of the corresponding molten salt are discussed. The effect of density changes in molten KI on these properties is discussed.

(*Received November 28, 1975*)

1 INTRODUCTION

Recently some results for the structure of molten alkali halides have appeared. Neutron scattering experiments on samples with different isotopic enrichments have been reported for NaCl by Edwards, Enderby, Howe and Page[1] and for KCl by Derrien and Dupuy.[2] In principle structure factors for three different enrichments allow one to determine the three partial radial distribution functions but, as Edwards *et al.* have discussed, the simultaneous equations which are used in this determination are extremely ill-conditioned. Edwards *et al.* have chosen their enrichments in a way which minimises this problem and question the reliability of the KCl work, attributing much of the fine structure found in that work to ill-conditioning and incorrect elimination of the scattering from the quartz container. Whereas the KCl experimental results bear very little comparison at all with the Monte Carlo results of Woodcock and Singer[3] using the potentials of Fumi and Tosi,[4] the NaCl results are in reasonable agreement with the molecular dynamics simulations of Lantelme, Turq, Quentrec and Lewis[5] based on potentials from the same source. Further careful experimental work will have to be carried out before we can be sure of the essential correctness of the picture of molten alkali halides as particles with charges $\pm e$ interacting via short range potentials in addition to the Coulombic potentials.

The main object of this paper is to investigate the range of possible results to be expected from various potentials which fall within this broad description. Only when a clear understanding of this point is available will it be

possible to point at certain features of experimental partial distribution functions as indicating departures from the picture e.g. clustering or covalency effects.

In another paper on NaI[6] we have investigated the effects of polarisation of the ions and found quite significant differences in the partial radial distribution functions from simulations with consistent rigid ion and shell model potentials. It was difficult to say how much of these differences arose directly from the introduction of polarisation and how much arose indirectly due to the implied change in ion sizes which results from going to a shell model from a rigid ion model. It might be thought that if a comparison was made between the results from a simulation using the Fumi-Tosi (rigid ion) potentials and those from a simulation with the same potentials augmented by some shell model parameters to take account of the polarisation then a clearer indication of the role of polarisation would be given. This has been carried out for KI by Jacucci, McDonald and Rahman[7] but, as will be discussed in the next section, this procedure does not treat properly the coupling between polarisation and the short range interactions.

In our work on NaI[6] the properties of diatomic molecules were used to determine the interionic potentials (in addition to solid state data). It is doubtful whether it is reasonable to assume that the same interaction potentials apply to molecules and solids. In particular at the molecular interionic distances the van der Waals part of the interaction must be seriously in question. When the same procedure is applied to KI the equations do not yield a (physical) solution. In this paper therefore we introduce a variant of the procedure for determining shell model potential parameters in which only solid state data is used. This method interprets the potentials in terms of the relative ion sizes. Results of simulations with a range of relative ion sizes will be presented.

In addition to investigating these ion size effects we shall study the effects on the static and dynamic properties of molten KI of varying the density of the melt.

2 INTERIONIC POTENTIALS

From work on lattice vibrations it is clear that the polarisation of ions plays a vital role in the dynamics of solids. (See, for example, the review by Cochran.[8]) The shell model has proved highly successful as a method of describing the polarisation and its coupling to the short range interactions, its success being judged mainly from the excellent agreement between calculated and measured phonon dispersion relations. It seems essential therefore in the description of molten systems via interionic potentials that the

ideas of the shell model (or some equivalent model) be incorporated. In view of the complexity and, more importantly, the heavy computer time requirements of simulations for ionic melts, the systems have to be represented by pairwise additive (central) potentials. This restriction, which is known from elastic constant measurements to be unrealistic, is not normally applied to solid state force constant models and this means that the dispersion curves resulting from our potentials will necessarily be less good than those from the more general shell model. In all cases which we have investigated including NaI[6] this has not proved serious. As in NaI we shall assume that the positive ion can be taken to be unpolarisable although this assumption will be less good for KI. From the electronic polarisabilities quoted by Kittel[9] the ratio I^-:K^+ is 8.5 with the Pauling[10] values and 4.8 with the Tessman, Kahn and Shockley[11] values whereas the corresponding ratios for NaI are 39.7 and 15.7. With this assumption the only shell parameters required are Y, the iodide shell charge in units of $|e|$, and k, the force constant between the shell and core of the I^- ion in units of $\frac{e^2}{V}$ where $V = 2a_0^3$ is the volume of the unit cell, a_0 being the nearest neighbour distance. These units are standard in lattice dynamics work and make Y and k dimensionless. In addition to these two parameters we require the parameters of the short range interaction potentials,

$$\phi_{ij}(r) = B_{ij} \exp(-\alpha_{ij} r) - C_{ij}/r^6 - D_{ij}/r^8 \qquad (1)$$

The van der Waals coefficients C_{ij} and D_{ij} are assumed to be those given by Mayer[12] and the parameters B_{ij} and α_{ij} in the short range repulsive terms, which are assumed to have the simple Born-Mayer form, remain to be determined. When the index i or j refers to the I^- ion the potential is taken to act through the shell centre, which is the usual assumption made in lattice dynamics work. The only other interactions involved are the Coulombic terms between cores and shells (excluding those between I^- shells and their own cores) and these interactions involve no new parameters.

The first step is to determine the shell parameters Y and k from the dielectric constants ϵ_0 and ϵ_∞, and follows our NaI work exactly. Expressions for the dielectric constants involve the nearest neighbour short range interaction ϕ_{+-} (in addition to the parameters Y and k) through a term R_0 where

$$\frac{e^2}{2V} R_0 = \left[\frac{d^2\phi_{+-}}{dr^2} + \frac{2}{r}\frac{d\phi_{+-}}{dr}\right]_{r=a_0}$$

$$= \alpha_{+-}(\alpha_{+-} - \frac{2}{a_0}) B_{+-} \exp(-\alpha_{+-} a_0) - 30C_{+-}/a_0^8 - 56D_{+-}/a_0^{10} \qquad (2)$$

In order to ensure the correct coupling of the polarisation to the short range terms we use, in addition to the dielectric constant expressions, the expressions, for the transverse optic frequency, ω_0, which again contains Y, k and R_0. In Table I we list the experimental values at 0° K for ϵ_0 from Lowndes[13], ϵ_∞ and ω_0 from Lowndes and Martin[14] and a_0 from Ghate.[15] The values of Y, k and R_0 obtained from these are also given.

It is at this stage that the potentials used by Jacucci *et al.*[7] are unphysical as the authors point out. They use potentials of the form of Eq. (1) with constants determined by Fumi and Tosi[4] and supplement this with values of Y and k determined by the above procedure but using slightly different values for the experimental input data.[16] The value of R_0 from the Fumi-Tosi potentials is $R_0 = 9.358$ and is therefore quite inconsistent with the value implied by the determination of Y and k. When this value of R_0 and the value of Y and k from the source which they quote[16] are substituted into the expressions for ϵ_0, ϵ_∞ and ω_0 the calculated values are in error by 40%, 1.5% and −21% respectively. From the Lyddane-Sachs-Teller[17] relation, the LO frequency at the zone centre $\left(= \omega_0 \left(\frac{\epsilon_0}{\epsilon_\infty}\right)^{1/2}\right)$ will be approximately correct but this is quite fortuitious.

This first stage therefore yields the parameters Y and k and a value of R_0 which provides a constraint on the + − potential parameters which from Eq. (2) may be written as

$$B_{+-} = \frac{\frac{e^2}{2V} R_0 + 30C_{+-}/a_0^8 + 56D_{+-}/a_0^{10}}{\alpha_{+-}(\alpha_{+-} - 2/a_0) \exp(-\alpha_{+-} a_0)} \tag{3}$$

In order to simplify the determination of the + + and − − interactions we make certain assumptions which, although they lack any real foundation, have been used by Fumi and Tosi[4] and in earlier work in this field. These

TABLE I

Input data and calculated values of I^- shell parameters in KI

Data	Parameters
$\epsilon_0 = 4.66$	$Y = -3.584$
$\epsilon_\infty = 2.684$	$k = 137.8$
$\omega_0 = 2.064 \times 10^{13}\ \text{sec}^{-1}$	$R_0 = 12.086$
$a_0 = 3.489$ Å	

are (a) that the exponents α_{ij} are all taken to be equal

$$\text{i.e. } \alpha_{+-} = \alpha_{++} = \alpha_{--} \equiv \alpha \tag{4}$$

and (b) that the premultiplying factors B_{ij} may be written in the form

$$B_{ij} = b\beta_{ij} \exp(\alpha(\sigma_i + \sigma_j)) \tag{5}$$

with b independent of the interaction type, β_{ij} the Pauling factors[18] ($\beta_{+-} = 1$, $\beta_{++} = 1.25$ and $\beta_{--} = 0.75$ for KI) and σ_i, σ_j the ionic radii.
We make the further assumption that

$$\sigma_+ + \sigma_- = a_0 \tag{6}$$

with assumptions (4) and (5) we immediately have the following relation between B_{++}, B_{--} and B_{+-}:

$$B_{++} \cdot B_{--} = \frac{15}{16} B_{+-}^2 \tag{7}$$

A further relationship between the premultiplying factors is obtained by imposing the condition that the total energy per unit cell be a minimum at the equilibrium ion separation. The total energy is taken to include long range coulombic terms, which are given in terms of the Madelung constant α_M, and nearest and second nearest neighbour short range terms from Eq. (1). After some rearrangement this condition may be written as

$$B_{++} + B_{--} = \frac{1}{6\sqrt{2}\alpha}\left[\frac{e^2}{a_0^2}(\alpha_M + \frac{3}{2}B) + \frac{6C}{a_0^7} + \frac{8D}{a_0^9}\right] \exp(\sqrt{2}\alpha a_0) \tag{8}$$

with

$$\frac{e^2}{2V}B = \left[\frac{1}{r}\frac{d\phi_{+-}}{dr}\right]_{r=a_0} \tag{9}$$

$$C = 0.75(C_{++} + C_{--}) \tag{10}$$

and

$$D = 0.375(D_{++} + D_{--}) \tag{11}$$

The procedure then is as follows:

(i) We choose a value of α
(ii) B_{+-} is obtained from Eq. (3) and using Eq. (5) and (6) we determine b
(iii) B is found from Eq. (9) using α and B_{+-} and the roots of the quadratic equation from (7) and (8) are found. Since for KI $\sigma_- > \sigma_+$ the roots may be identified ($B_{--} > B_{++}$ from equation (5)).
(iv) Using these values for B_{++} and B_{--} and the known value for b Eq. (5) yields the ionic radii σ_+ and σ_-.

Table II shows the results of these calculations with $\alpha = 3.2$, 3.6 and 4.0. In Table III are listed some sets of ionic radii from other sources. These are not constrained to satisfy Eq. (6) although the agreement in all cases is fairly

TABLE II

Short range parameters for KI

Run		3/4/5	1	2
α	Å^{-1}	3.2	3.6	4.0
B_{+-}	$\times 10^{-12}$ erg	1.500×10^4	4.672×10^4	1.499×10^5
B_{++}	$\times 10^{-12}$ erg	6.301×10^3	1.754×10^3	1.746×10^3
B_{--}	$\times 10^{-12}$ erg	3.347×10^4	1.167×10^6	1.211×10^7
σ_+	Å	1.5741	1.2576	1.1600
σ_-	Å	1.9149	2.2314	2.3290

TABLE III

Collected estimates of ionic radii

Source	Reference	σ_+(Å)	σ_-(Å)
Fumi and Tosi 1st set	4	1.463	1.907
Fumi and Tosi 2nd set	4	1.554	2.013
Zachariasen (Kittel)	9	1.33	2.19
Pauling (Kittel)	9	1.33	2.16

close. A comparison shows that values of α between 3.2 and 3.6 would gi agreement with any of these sets. The case with $\alpha = 4.0$ will indicate wh effects are to be expected when the size of the positive ion is reduce

We shall not show the dispersion relations obtained from these mod as the level of agreement with experiment is similar to that found in N and is quite satisfactory for our purpose. Indeed this is almost guarante by fitting to ϵ_0, ϵ_∞ and ω_0. The gradients of the acoustic branches ne the zone centre are related to the elastic constants. Table IV gives the valu calculated from the three models together with the low temperatu measurements of Norwood and Briscoe.[19] The equality of C_{12} and C_{44} i consequence of our central potential assumption (the Cauchy relation). no case is the agreement very good but the results indicate that the low value of α is the most physical, a conclusion which is in keeping with the ior

TABLE IV

Experimental and calculated elastic constants for KI at 0°K

	C_{11}	C_{12}	C_{44}
	$\times 10^{12}$ dyn/cm^2		
Experiment	0.338	0.022	0.0368
$\alpha = 3.2$ Å^{-1}	0.3678	0.0528	0.0528
$\alpha = 3.6$ Å^{-1}	0.4169	0.0885	0.0885
$\alpha = 4.0$ Å^{-1}	0.4679	0.1225	0.1225

radii predictions. From the trends in Table IV it is clearly tempting to try a lower value of α but when this is attempted the procedure breaks down at step (iii).

3 MOLECULAR DYNAMICS SIMULATION

The methods used follow those which we have already reported in our work on NaI[6] and will not be discussed here. Simulations were carried out with N^+ positive and N^- negative ions in a cubic box of side L. Values of the controlling parameters for the various runs are listed in Table V. Periodic boundary conditions were used to provide an approximation to the bulk of the liquid. The Coulombic forces were calculated using the Ewald transformation to include all periodic images. The short range forces were truncated on a sphere of radius L/2. Randomised configurations were used to start the simulations and the equations of motion were integrated numerically with steps Δt. In each case the system was allowed to equilibrate for N_{equil} time steps before the statistical quantities of interest were accumulated over the following N_{run} time steps. The average temperatures $\langle T \rangle$ were calculated from the kinetic energy of the ions. The average pressures $\langle P \rangle$ were obtained by using the virial expression and assuming that the partial radial distribution functions are unity for $r > L/2$. The total energy which should be constant for a microcanonical ensemble was stable with the maximum fluctuations being $\pm 0.07\%$. No major drift in temperature was found indicating that the time steps were sufficiently small and that the procedure which we use for relaxing the shells is stable. It was therefore not necessary to resort to a velocity rescaling procedure such as that used by Jacucci *et al.*[7] During the simulations we observe that a non-negligible number of ions are quite strongly polarised with separations of the shell centres from the cores of up to 0.3 Å.

As we expected that the changes in properties due to ion size effects would be larger than those due to density changes a larger number of ions was used in the simulations where we look for more subtle effects.

TABLE V

Controlling parameters in simulation runs

RUN	1	2	3	4	5
$N^+ = N^-$	32	32	108	108	108
L (Å)	16.0	16.0	24.0	22.0	26.0
$\langle T \rangle$ (°K)	1249	1282	1273	1317	1377
$\langle P \rangle$ (Kbar)	1.5	2.5	1.0	10.	−0.5
Δt ($\times 10^{-15}$ sec)	6.3	6.3	6.3	5.5	6.1
N_{equil}	450	450	150	150	150
N_{run}	1550	1550	1050	1050	1050

4 RADIAL DISTRIBUTION FUNCTIONS

The radial distribution functions for five simulations are shown in Figure 1 and a summary of the positions and values of maxima and minima is given in Table VI. The labelling of the simulation runs corresponds with that used in Tables II and V. The set 1, 2 and 3 is used to investigate ion size effects and the set 3, 4 and 5 (each of which has the same short range potential) looks at the effects of varying the density. Since the I^- ion is represented by a shell and a core, there are functions corresponding to each of these "particles". In our NaI work[6] we distinguished between these but here only core functions are plotted. (Since the cores contain the nuclei these are the distribution functions appropriate to neutron scattering experiments.)

Firstly we shall draw attention to some of the features which emerge from Figure 1 and Table VI for the first three simulations. Taken in the order 3 to 1 to 2 these show the effects of hardening the short range potentials (by increasing the value of α) and consequently of increasing the ion-size ratio $\sigma_- : \sigma_+$.

(a) The first peak in g_{+-} does not change in position but the peak height increases as the ratio $\sigma_- : \sigma_+$ (or α) is increased. The first minimum shows a slight variation in position, which is probably not significant, but little variation in value. The second maximum has very similar positions and values in all three cases, so that the major difference is only around the first peak.

(b) The main differences in g_{++} are again in the region of its first peak. As α and the ratio $\sigma_- : \sigma_+$ are increased the first peak is depressed and comes at successively lower separations. Consistent with σ_+ taking smaller values the distance of closest approach also decreases as we go through the sequence. (3.2 Å, 3.0 Å and 2.8 Å.)

(c) The most marked changes are found in g_{--}, notably the change in the height of the first peak. Since the peak is wide this constitutes a major change in the structure. Again the distance of closest approach is consistent with the ion size: as we go through the sequence increasing σ_- (and α) the approach distance increases from 3.2 Å through 3.7 Å to 3.9 Å.

(d) Although peak heights and positions for g_{++} and g_{--} are not well defined it is clear that the functions are well separated and this becomes more emphasized as the ion sizes become different. Further, in simulation 3 (which includes more particles) this separation persists out to 12 Å.

We shall now highlight some of the more important consequences of increasing the density i.e. decreasing the box size L. These can be seen by comparing the results of the final three simulations, the density being increased as we go through the sequence 5 to 3 to 4.

(a) The first peak in g_{+-} again shows no change in position but the peak height decreases with increasing density. As the density increases the sub-

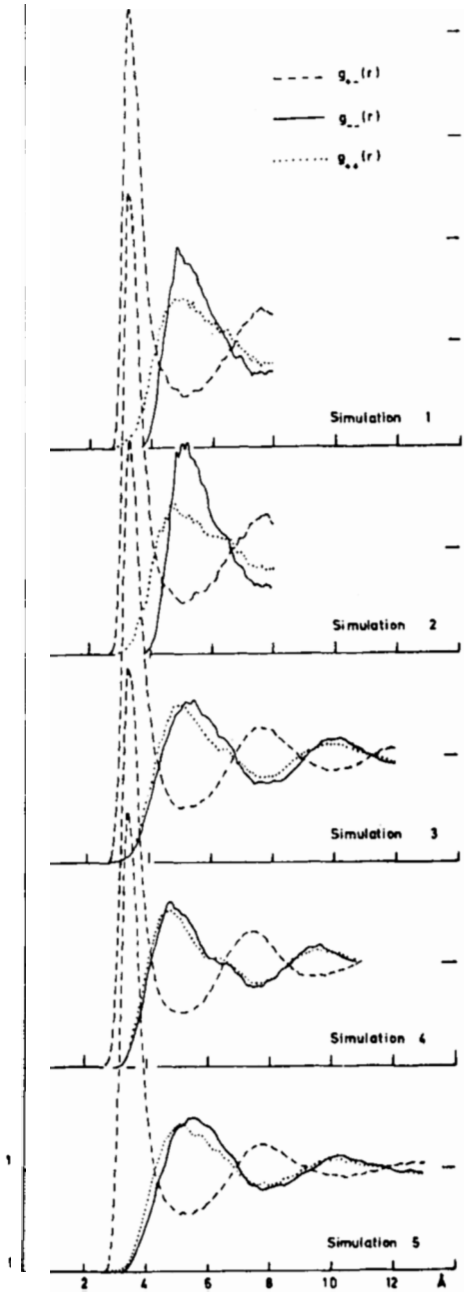

FIGURE 1 Partial radial distribution functions for the five simulations.

TABLE VI

Positions (in Å) and values of features in radial distribution functions

Function	Feature	Simulations 1	2	3	4	5
g_{+-}	First maximum					
	Value	4.29	4.50	4.11	3.89	4.48
	Position	3.3	3.3	3.3	3.3	3.3
	First minimum					
	Value	0.48	0.48	0.50	0.50	0.54
	Position	5.2	5.1	5.0	5.2	5.0
	Second maximum					
	Value	1.32	1.34	1.28	1.31	1.22
	Position	7.6	7.8	7.6	7.4	7.8
	Second minimum					
	Value			0.86	0.86	0.90
	Position			10.0	9.4	10.4
g_{++}	First maximum					
	Value	1.44	1.40	1.49	1.52	1.44
	Position	5.1	4.8	5.3	4.7	5.1
	First minimum					
	Value	0.82	0.78	0.80	0.80	0.83
	Position	7.8	7.8	7.8	7.6	7.8
	Second maximum					
	Value			1.11	1.16	1.08
	Position			10.0	9.6	10.2
g_{--}	First maximum					
	Value	1.96	2.04	1.55	1.60	1.48
	Position	4.9	5.1	5.4	4.7	5.4
	First minimum					
	Value	0.70	0.62	0.75	0.76	0.78
	Position	7.6	7.6	7.8	7.5	7.8
	Second maximum					
	Value			1.16	1.15	1.11
	Position			10.0	9.2	10.3

sequent maxima and minima become more emphasised and move to smaller interionic separations. It must be assumed that the irregularity between 5.0 Å and 5.6 Å in simulation 3 is due to poor statistics and is not related to the feature which Edwards *et al.*[1] observe for NaCl at an equivalent position. (The feature is not present in simulations 4 and 5.)

(b) The clear separation of g_{++} and g_{--} at the lower densities becomes much less marked at the highest density. Although both curves oscillate with greater amplitude and have maxima and minima at smaller separations as the density is increased, it is g_{--} which displays the greater response to this change. This is particularly significant around the first maximum.

(c) As density is increased g_{++} and, to a lesser extent, g_{--} develops shoulders at a separation of around 6.4 Å. (More extensive calculation would be required to confirm that this is not due to poor statistics.) A similar feature has been observed experimentally in NaCl by Edwards *et al.*[1] although this seems to be correlated with their feature in g_{+-} mentioned above. Copley and Rahman[20] have observed shoulders in g_{++} and g_{--} in their Molecular Dynamics simulation of RbBr while Jacucci *et al.*[7] report a definite kink in g_{++} and a lesser one in g_{--} in a similar range for KI. Since our simulations were started from a very well randomised liquid configuration we do not believe that this shoulder represents a memory of an initial crystal lattice but conclude that it is a feature of the melt.

5 VELOCITY AUTO-CORRELATION FUNCTIONS

The normalised velocity auto-correlation functions are defined by

$$\phi_{\pm}(t) = \frac{\Sigma \mathbf{v}_i(0) \cdot \mathbf{v}_i(t)}{\Sigma \mathbf{v}_i(0) \cdot \mathbf{v}_i(0)}$$

where the summations are carried out over all the positive or negative ions. In constructing these functions we average over 100 different time origins at intervals of $10\Delta t$. The work on NaI[6] indicated that the introduction of polarisation produces major changes in the characteristics of the velocity autocorrelation functions: it is reasonable to expect larger changes in dynamic properties than in static properties such as the radial distribution functions discussed above. In this paper we examine the changes which arise as the short range potential is varied (simulations 1, 2 and 3) and as the density is changed (simulations 3, 4 and 5).

Since the functions for all five simulations are broadly similar we only show the functions for one simulation (No. 3) in Figure 2 and list in Table VII the following characteristic values for all the simulations:

i) the time after which the function first decays to zero
ii) the depth of the anti-correlation bowl
and iii) the time to reach the minimum of this bowl.

As the ion size ratio is changed (with the negative ion size increasing as we go through the sequence 3 to 1 to 2) much larger changes are found in $\phi_-(t)$ than in $\phi_+(t)$, which remains remarkably constant. As σ_- is increased $\phi_-(t)$ is condensed in towards the time origin which is consistent with the expected higher collision diameter.

Increasing the density (simulation 5 to 3 to 4) produces quite pronounced changes in both velocity auto-correlation functions. The times for reaching

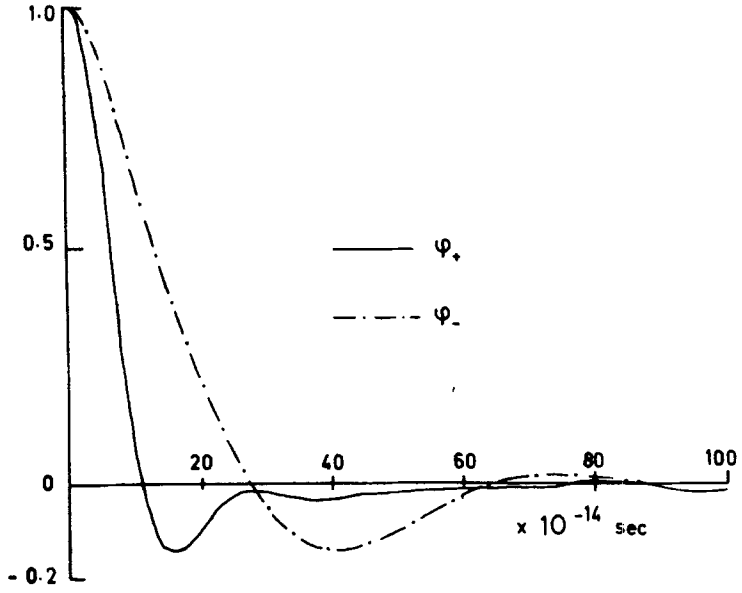

FIGURE 2 Normalised velocity autocorrelation functions for simulation 3.

TABLE VII

Times (in units of 10^{-14} sec) and values of characteristic features of velocity auto-correlation functions.

Function	Feature	Simulations 1	2	3	4	5
ϕ_+	Zero	11	11	11	9	13
	Bowl Depth	−0.14	−0.12	−0.14	−0.21	−0.06
	Time to reach minimum	15	15	17	14	17
ϕ_-	Zero	23	20	27	22	36
	Bowl depth	−0.19	−0.18	−0.14	−0.22	−0.05
	Time to reach minimum	36	34	40	36	48

zero and the minimum become significantly shorter and the depths of the anti-correlation bowls increase considerably. This is consistent with the decreasing ability of ions to diffuse in a denser liquid and the consequent emphasis of vibratory behaviour.

6 FORCE AUTO-CORRELATION FUNCTIONS

The definition of the normalised force auto-correlation functions $\psi_{\pm}(t)$ is similar to that for the velocity functions with particle velocities replaced by accelerations. Again we only show full results for one case (simulation 3) in Figure 3 and list some characteristic values for all the simulations in Table VIII. For ψ_+ we list the times for the first and second crossings through zero, the time to reach the minimum and the value at this minimum. The functions ψ_- show a double minimum and further characteristic values are given to specify this feature. Since there is considerable detailed variation in ψ_- around this double minimum between simulations we have indicated this in the inset which is on the same scale as the main figure.

The function ψ_+ shows very little systematic change as the potential is varied (1, 2 and 3) but as the density is increased (5 to 3 to 4) the depth of

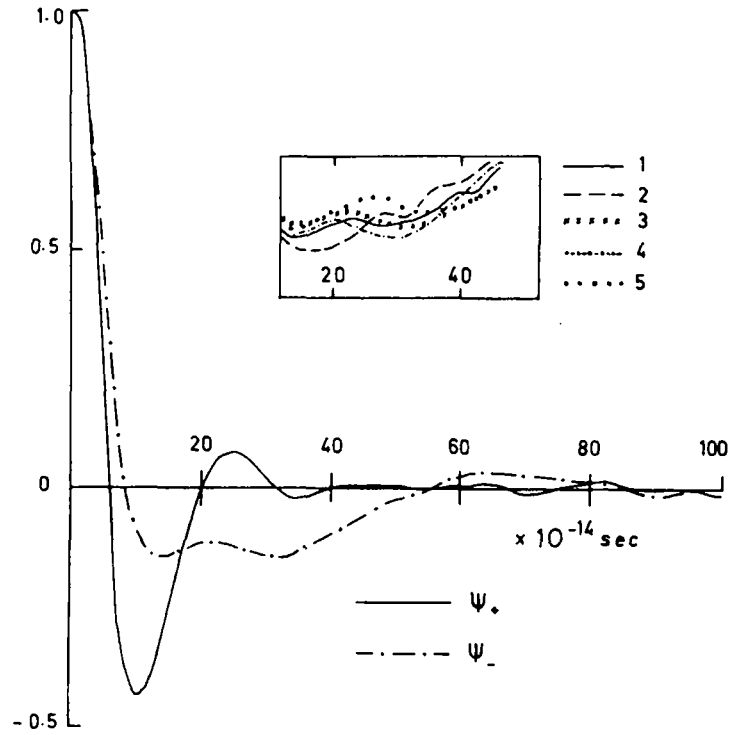

FIGURE 3 Normalised force autocorrelation functions for simulation 3. The inset shows the variations in the region of the double minimum of ψ_- for the five simulations (on the same scale).

the bowl increases and the function returns to zero at successively shorter times.

As is the case with the velocity functions the negative ion function ϕ_- displays a stronger response to changes in the ion size ratio. As the negative ion size is increased (3 to 1 to 2) the first minimum becomes progressively deeper and the function returns to zero at progressively shorter times, both properties again being consistent with the increasing constraints as the ion becomes larger. As the density is increased (5 to 3 to 4) the times become shorter, notably those for the second minimum and the return to zero; also

TABLE VIII

Times (in units of 10^{-14} sec) and values of characteristic features of acceleration auto-correlation functions.

Function	Feature	Simulations 1	2	3	4	5
ϕ_+	Zero	6	6	6	6	7
	Bowl depth	−0.44	−0.39	−0.44	−0.48	−0.40
	time	11	9	11	9	10
	Zero	19	20	20	18	22
ϕ_-	Zero	9	8	8	8	8
	Bowl depth	−0.17	−0.20	−0.15	−0.17	−0.16
	time	14	16	14	14	14
	Bowl depth	−0.15	−0.13	−0.15	−0.17	−0.12
	time	27	30	32	29	33
	Zero	49	45	56	48	60

the second minimum becomes more pronounced. As in the velocity functions this is consistent with the decreasing ability to diffuse as the density is increased.

7 MEAN SQUARE DISPLACEMENTS OF IONS

The mean square displacements of ions are defined by

$$\langle r(t)^2 \rangle_\pm = \frac{1}{N^\pm} \sum \left[r_i(t) - r_i(0) \right]^2$$

with summations and time averaging as in the velocity auto-correlation functions. These functions are shown for all the simulations in Figure 4. All the curves show the same general features, an initial concave section followed by a convex section leading to the linear section. The lighter ion goes through this sequence more rapidly than the heavy one.

It is difficult to make direct comparisons between the curves because

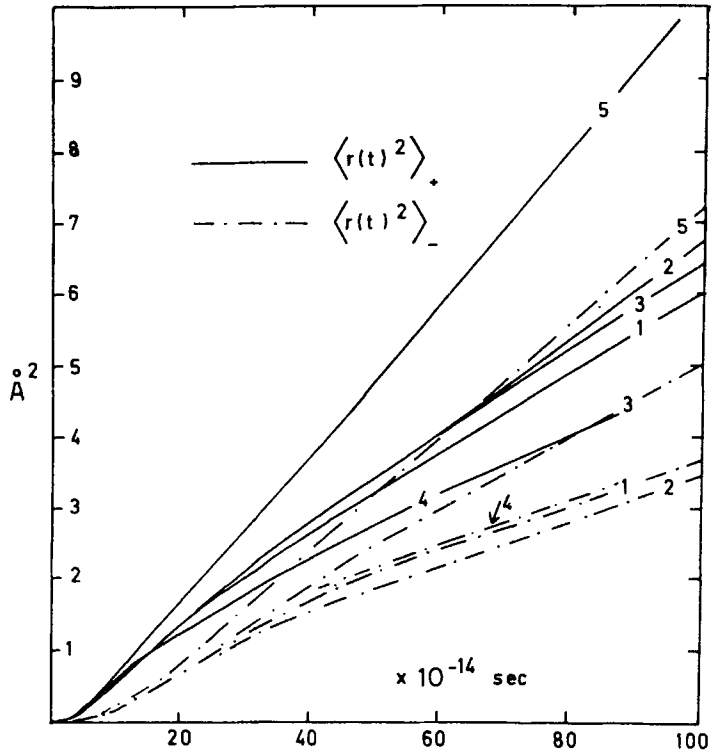

FIGURE 4. Mean square displacements of ions for the five simulations.

in the linear regime the gradient is related to the self-diffusion coefficient which depends exponentially on temperature. Since in a microcanonical ensemble temperature is a fluctuating quantity its average value cannot be fixed in advance of a simulation run. However in simulations 2 and 3 the average temperatures agree to about 1% and valid comparisons can be made. Decreasing the size of the positive ion produces little change in either the concave or convex regimes and it is only after about 65×10^{-14} sec. that any difference becomes apparent: the difference is such that the smaller ion has a slightly higher diffusion coefficient. In contrast making the negative ion larger decreases the mean square displacement significantly in the concave and convex regimes as well as the linear one.

Although the average temperature of simulation 3 is 4% less than that for simulation 4 we can still make some useful comparisons since increasing the temperature would make the particles mobile while increasing the density would tend to restrict mobility. Thus a comparison will underestimate the effects of the change in density. It is clear that both ions are

considerably more mobile at the lower density (simulation 3): in fact after 80×10^{-14} sec. the iodide ion in simulation 3 has a larger mean square displacement than the potassium ion in simulation 4. This provides support for the suggestion made concerning the auto-correlation functions namely that as the density is lowered the diffusion process becomes much more effective at dissipating the vibratory motion of the ions.

References

1. F. G. Edwards, J. E. Enderby, R. A. Howe and D. I. Page, *J. Phys. C: Solid St. Phys.* **8**, 3483, (1975).
2. J. Y. Derrien and J. Dupuy, Journal de Physique **36**, 191, (1975).
3. L. V. Woodcock and K. Singer, J.C.S. Faraday II, **67**, 12 (1971).
4. M. P. Tosi and F. G. Fumi, *J. Phys, Chem. Solids* **25**, 45 (1964).
5. F. Lantelme, P. Turq, B. Quentrec and J. W. E. Lewis *Mol. Phys.* **28**, 1537 (1975).
6. M. Dixon and M. J. L. Sangster, *J. Phys. C: Solid St. Phys.* **8**, L8 (1975), and *J. Phys. C: Solid St. Phys.* **9**, 909 (1976).
7. G. Jacucci, I. R. McDonald and A. Rahman, *Phys. Rev.* (to be published).
8. W. Cochran, C. R. C. Critical Reviews in Solid State Sciences **2**, 1 (1971).
9. C. Kittel "Introduction to Solid State Physics" 2nd Edition (Wiley: N. York and London) (1956).
10. L. Pauling, *Proc. Roy. Soc.* **A114**, 181 (1927).
11. J. R. Tessman, A. H. Kahn and W. Shockley, *Phys. Rev.* **92**, 890 (1953).
12. J. E. Mayer *J. Chem. Phys.* **1**, 270 (1933).
13. R. P. Lowndes, Physics Letters, **21**, 26 (1966).
14. R. P. Lowndes and D. H. Martin, *Proc. Roy. Soc.* **A308**, 473, (1969).
15. P. B. Ghate, *Phys. Rev.* **139**, A1666 (1965).
16. M. J. L. Sangster, *J. Phys. Chem. Solids* **34**, 355 (1973).
17. R. H. Lyddane, R. G. Sachs and E. Teller, *Phys, Rev.* **59**, 673 (1941).
18. L. Pauling, *Z. Krist.* **67**, 377 (1928) and J. A. C. S. **50**, 1036 (1928).
19. M. H. Norwood and C. V. Briscoe, *Phys. Rev.* **112**, 45 (1958).
20. J. R. D. Copley and A. Rahman, submitted to *Phys, Rev.*